CONF-770692--1

MASTER

PREPRINT UCRL-80121

Lawrence Livermore Laboratory

NUMERICAL STUDY OF PARTICLE MOTION IN TWO WAVES

Gary R. Smith

September 9, 1977

This paper was prepared for submission to the Proceedings of the International Conference on "Stochastic Behavior in Classical and Quantum Hamiltonian Systems," held in Como, Italy, June 20-24, 1977.

NUMERICAL STUDY OF PARTICLE MOTION IN TWO WAVES

Gary R. Smith

Lawrence Livermore Laboratory
University of California
Livermore, CA 94550

September 9, 1977

ABSTRACT

We are studying the dynamical system described by the Hamiltonian $H = H_0 + \epsilon V$, where

$$H_0 = \frac{1}{2} p^2 - \cos x, \quad V = - \cos (\lambda x - \Omega t).$$

We have encountered this system in a number of problems of practical importance. In addition, the system has intrinsic interest for the theory of adiabaticity and stochasticity. The invariant action J of the unperturbed Hamiltonian H_0 is subject to strong modification or destruction because of the perturbation ϵV. Absence of an invariant (i.e., stochasticity) occurs in a phase space region whose size and shape vary with the three parameters ϵ, λ, Ω. Previous studies have varied the amplitude of a perturbation (our ϵ); we emphasize here the strong dependences on the space (λ) and time (Ω) scales of the perturbation. Our results show that a perturbation is most effective at causing stochastic motion if its space and time scales are comparable (λ~1, Ω~1) to those in the unperturbed Hamiltonian H_0.

1. INTRODUCTION

Much study has been devoted to the Hénon - Heiles Hamiltonian, which we write in the form

$$H = \left(p_x^2 + p_y^2\right)/2m + \frac{1}{2} k(x^2 + y^2) + \epsilon\left(x^2 y - \frac{1}{3} y^3\right). \qquad (1)$$

It is customary to eliminate the constants m, k, and ϵ by using a set of units in which

unit of mass = m

unit of length = k/ϵ

unit of time = $(m/k)^{1/2}$

unit of energy = k^3/ϵ^2.

A particle of given dimensional energy C, moving in a well with a given k, has a large value of the dimensionless energy $E = C\epsilon^2/k^3$ if ϵ is large. The onset of stochasticity[1] as E is increased is thus caused by the increasing amplitude ϵ of the perturbation in (1).

More generally, the space and time scales of a perturbation, in addition to its amplitude, can be important in determining the onset of stochasticity. A dynamical system which displays these properties is given by

$$H(x,p,t) = H_0 (x,p) + \epsilon V(x,t), \qquad (2)$$
$$H_0 = \frac{1}{2} p^2 - \cos x, \qquad V = -\cos (\lambda x - \Omega t).$$

This system occurs in several problems in plasma physics, ranging from purely theoretical problems[2-4] through a modest laboratory experiment[5] to studies of interest to the important fusion energy program[6-8]. Hamiltonian (2) occurs frequently because many problems can be reduced to the motion of a particle in a one-dimensional potential which varies periodically in space and time. Fourier analysis of the potential yields, in general, a large number of sinusoidal terms. Sometimes all but two of these terms can be ignored, resulting in (2). We view this dynamical system as an elementary problem in stochasticity theory which exhibits features seen in many, more complicated problems. We use the phrase "particle motion in two waves" to describe (2).

2. HAMILTONIAN IN ACTION-ANGLE VARIABLES

In preparation for the presentation below of our numerical results, we introduce the variables which are most convenient in theoretical work. *These are the action and angle variables of the unperturbed Hamiltonian* H_0. Since H_0 describes the well-known (nonlinear) pendulum problem, one expects elliptic integrals and Jacobian elliptic functions to appear. In the notation of Ref. 9 the definitions of the action J and of the angle ϕ are

$$J(H_0) = \frac{8}{\pi}\left[E(\kappa) - (1-\kappa^2)\, K(\kappa)\right]$$

$$\phi(x,H_0) = \pi\, F(\zeta,\kappa)/2\, K(\kappa),$$

where $\kappa \sin \zeta = \sin \frac{1}{2} x$, and where the modulus k is given by

$$\kappa^2 = \frac{1}{2}(1 + H_0).$$

These definitions are valid only for a particle which has $H_0 < 1$ and is therefore trapped in the unperturbed potential well. Our definitions for an untrapped particle are available in Ref. 10.

The action-angle variables are convenient because the unperturbed motion is described so simply in terms of them:

$$\dot{J} = -\partial H_0/\partial\phi = 0 \Rightarrow J = J(t=0)$$

$$\dot{\phi} = \partial H_0/\partial J \equiv \omega_b(J) = \text{const} \Rightarrow \phi = \phi_0 + \omega_b t$$

In terms of J and ϕ, the Hamiltonian appears

$$H(\phi,J,t) = H_0(J) + \varepsilon V(\phi,J,t) \tag{3a}$$

$$V = \sum_{n=-\infty}^{\infty} V_n(J,\lambda)\cos(n\phi - \Omega t). \tag{3b}$$

The Fourier coefficients are given by

$$V_n = \frac{1}{2\pi}\int_{-\pi}^{\pi} d\phi \cos[\lambda x(\phi,J) - n\phi].$$

Expressions for $V_n\left(J,\ \lambda = \frac{1}{2}\right)$ are available in standard references, including Ref. 9. For half-integral values of λ (like $1, \frac{3}{2}, 2, \ldots$), the coefficients V_n can be computed by contour integration. The expressions *obtained from* reference works or by contour integration are valid for all J but only certain λ. On the other hand, it is very simple to find the approximate formula

$$V_n[J(k),\ \lambda] \approx J_n(2k\lambda), \tag{4}$$

valid for any λ, but accurate only for small values of κ. *The Bessel* function J_n on the right-hand side of (4) should not be confused with the action J on the left-hand side.

Our numerical results will show the presence of certain resonances (called bounce resonances) which are evident in (3). The nth term in (3b) has a large effect on the motion when it varies slowly in time:

$$n\dot{\phi} - \Omega \approx n\,\omega_b - \Omega \approx 0.$$

Chains of islands will be observed near the resonant values of the action J, which are defined by

$$n\omega_0(J) = \Omega \, . \tag{5}$$

3. NUMERICAL METHODS

Our study of the dynamical system (2) proceeds by numerical integration of the Hamiltonian equations of motion

$$\dot{x} = p, \; \dot{p} = -\sin x - \epsilon \lambda \sin(\lambda x - \Omega t) \, .$$

We make stroboscopic plots, analogous to Poincaré surface of section maps, by recording a point whenever $\Omega t = 2\pi N$, N=0,1,2,.... The recorded points are plotted not in the xp-plane, but in the ϕJ-plane. Since the unperturbed (ϵ=0) motion results in points on a horizontal line in the ϕJ-plane, our plots are particularly useful for seeing the effects of the perturbation.

4. *DISCUSSION OF RESULTS*

We keep the amplitude of the perturbation fixed at ϵ = 0.2 and study the motion for various λ and Ω. As a reference case we choose $\lambda = \Omega = 1$.

First, we consider the results of Fig. 1, for which λ is varied while Ω is kept equal to unity. In each part of the figure we show trajectories commencing at several different initial points in the ϕJ-plane. Initial points lying in the stochastic region of the plane lead to a set of trajectory points which cannot be connected by a smooth curve. Such trajectories indicate the absence of an isolating constant of the motion. Initial points lying in the nonstochastic parts of the ϕJ-plane lead to sets of trajectory points which have been connected by smooth curves.

The four plots in Fig. 1 dramatically show the growth of the stochastic region as λ is increased from much less than unity to the reference case of $\lambda = 1$. The prominent island in each plot is due to the bounce resonance (5) with $n = 1$. Notice how the features on the plots change size and shape as λ varies but do not move around much.

In Fig. 2 we keep λ equal to unity and choose four different values of Ω. The four plots in Fig. 2, together with the reference case ($\lambda=\Omega=1$) in Fig. 1, demonstrate that the largest stochastic region occurs for $\Omega=1$. In contrast to Fig. 1, the features on the plots of Fig. 2 move around rapidly as Ω is varied. As a result, different features are seen in each part of Fig. 2. As indicated in the figure caption, we attribute the chains of islands to particular resonances of the form $n\omega_b = m\Omega$, where n and m are positive integers. The appearance of such prominent islands with $m \neq 1$ was unexpected. Description of these islands will require a different theoretical formulation than that given in (3).

To graphically display the variations in size of the stochastic part of phase space we have devised a quantitative measure of the size. Our measure is definite, but admittedly arbitrary. For Figs. 1 and 2 we attempted to locate nonstochastic trajectories as close as possible to the separatrix, the horizontal line at $J = 8/\pi \approx 2.55$. The area of the ϕJ-plane between the separatrix and the "closest" trajectory is divided by the area of the plane bounded by $J = 0$ and $8/\pi$ and by $\phi = 0$ and 2π. We refer to the ratio as the "stochastic fraction". In Figs. 3 and 4 we plot our measurements of the stochastic fraction as a function of λ and Ω. The curves connecting the measured points are merely aids to the eye; a theoretical expression for the stochasitc fraction as a function of c, λ, and μ is not available.

Besides being visually pleasing, the plots in Figs. 1 and 2 suggest that the simple dynamical system (2) has many intriguing properties. Interesting results should be obtained by theoretical and numerical work extending that begun here.

Work performed under the auspices of the U.S. Energy Research and Development Administration under contract No. W-7405-Eng-48.

REFERENCES

1. M. Hénon and C. Heiles, Astron. J. 69, 73 (1964).

2. G. M. Zaslavskii and N. N. Filonenko, Zh. Eksp. Teor. Fiz. 54, 1590 (1968) [Sov. Phys. - JETP 27, 851 (1968)]. Particle in two waves.

3. P. K. Kaw and W. L. Kruer, Phys. Fluids 14, 190 (1971). Particle in two waves.

4. G. R. Smith and A. N. Kaufman, Phys. Rev. Lett. 34, 1613 (1975). Particle in a uniform magnetic field and a single, oblique wave.

5. G. Dimonte and J. H. Malmberg, Phys. Rev. Lett. 38, 401 (1977). Electron in two waves propagating on a traveling wave tube.

6. A. B. Rechester and T. H. Stix, Phys. Rev. Lett. 36, 587 (1976). Magnetic braiding in a tokamak.

7. M. Dobrowolny, A. Orefice, and R. Pozzoli, Plasma Phys. 16, 479 (1974). Particle in a tokamak magnetic field and a single wave.

8. G. R. Smith, Phys. Rev. Lett. 38, 970 (1977). Particle in a tokamak magnetic field and a single wave.

9. P. F. Byrd and M. D. Friedman, Handbook of Elliptic Integrals for Engineers and Scientists (Springer-Verlag, New York, 1971).

10. G. R. Smith, Ph.D. Thesis, University of California, Berkeley, Sept. 1977, LBL-6824 (unpublished).

FIGURE CAPTIONS

Fig. 1. Stroboscopic plots of particle trajectories, illustrating changes in the motion as λ is varied. The parameters $\epsilon = 0.2$ and $\Omega = 1$ are kept fixed. The initial points for the trajectories are marked by X's, and each initial point represents a particle trapped in the unperturbed potential at $t = 0$. The horizontal line at $J \simeq 2.55$ is the separatrix which divides trapped particles from untrapped ones.

Fig. 2. Stroboscopic plots illustrating changes in the particle motion as Ω is varied. The fixed parameters are $\epsilon = 0.2$ and $\lambda = 1$. The chains of islands seem to be due to the folowing resonances: the plot for $\Omega = 0.25$ shows $\omega_b = 3\Omega$, $\Omega = 0.5$ shows $3\omega_b = 5\Omega$, $\Omega = 2$ shows $2\omega_b = \Omega$ and $7\omega_b = 3\Omega$, and $\Omega = 4$ shows $5\omega_b = \Omega$.

Fig. 3. The stochastic fraction as a function of λ for $\epsilon = 0.2$ and $\Omega = 1$.

Fig. 4. The stochastic fraction as a function of Ω for $\epsilon = 0.2$ and $\lambda = 1$.

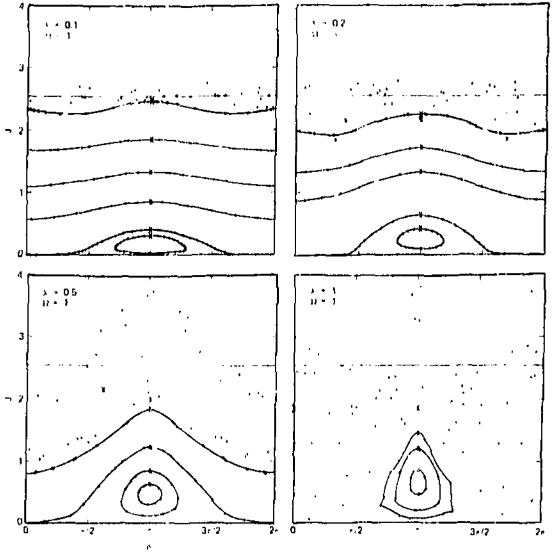

Figure 1

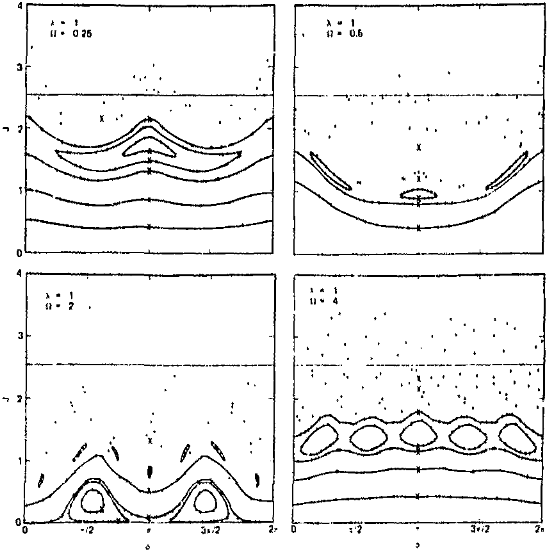

Figure 2

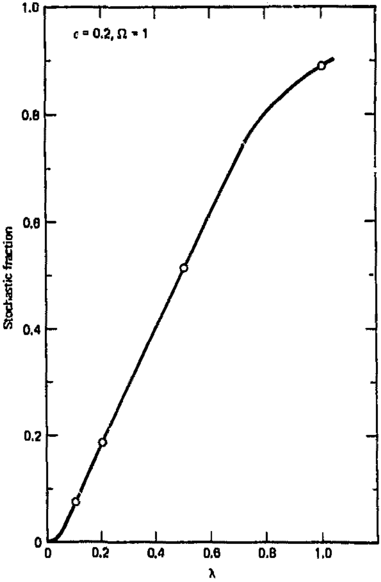

Figure 3

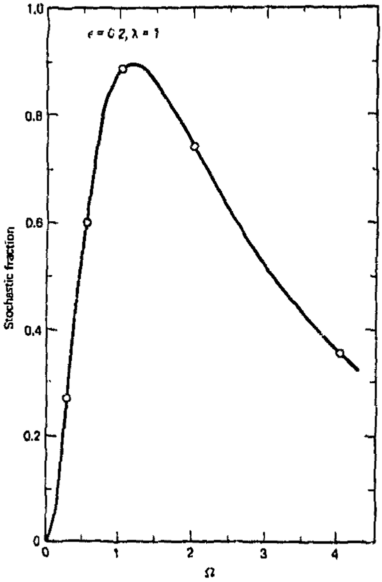

Figure 4